Two middle Pleistocene glacial-interglacial cycles from the Valle Grande, Jemez Mountains, northern New Mexico

Peter J. Fawcett, Heikoop. Jeff, Fraser Goff, R. Scott Anderson, Linda Donohoo-Hurley, John W. Geissman, Giday Woldegabriel, Craig D. Allen, Catrina M. Johnson, Susan J. Smith, and Julianna Fessenden-Rahn

2007, pp. 409-417. https://doi.org/10.56577/FFC-58.409

in:

Geology of the Jemez Region II, Kues, Barry S., Kelley, Shari A., Lueth, Virgil W.; [eds.], New Mexico Geological Society 58 th Annual Fall Field Conference Guidebook, 499 p. https://doi.org/10.56577/FFC-58

This page is intentionally left blank to maintain order of facing pages.

TWO MIDDLE PLEISTOCENE GLACIAL-INTERGLACIAL CYCLES FROM THE VALLE GRANDE, JEMEZ MOUNTAINS, NORTHERN NEW MEXICO

PETER J. FAWCETT[1], JEFF HEIKOOP[2], FRASER GOFF [1], R. SCOTT ANDERSON[3], LINDA DONOHOO-HURLEY[1], JOHN W. GEISSMAN[1], GIDAY WOLDEGABRIEL[2], CRAIG D. ALLEN[4], CATRINA M. JOHNSON[1], SUSAN J. SMITH[3], AND JULIANNA FESSENDEN-RAHN[2]

[1]Department of Earth & Planetary Sciences, University of New Mexico, Albuquerque, NM, 87131, fawcett@unm.edu

[2]Earth and Environmental Sciences Division, EES-6, Los Alamos National Laboratory, Los Alamos, NM, 87545

[3]Center for Environmental Sciences and Education, Northern Arizona University, Flagstaff, AZ 86001

[4]U.S.G.S. Fort Collins Science Center, Jemez Mountains Field Station, Los Alamos, NM 87544

Abstract — A long-lived middle Pleistocene lake formed in the Valle Grande, a large moat valley of the Valles caldera in northern New Mexico, when a post-caldera eruption (South Mountain rhyolite) dammed the drainage out of the caldera. The deposits of this lake were cored in May 2004 (GLAD5 project, hole VC-3) and 81 m of mostly lacustrine silty mud were recovered. A tentative chronology has been established for VC-3 with a basal tephra Ar-Ar date of 552 +/- 3 ka, a correlation of major climatic changes in the core with other long Pleistocene records (deep sea oxygen isotope records and long Antarctic ice core records), and the recognition of two geomagnetic field polarity events in the core which can be correlated with globally recognized events. This record spans a critical interval of the middle Pleistocene from MIS 14 (552 ka) to MIS 10 (~360 ka), at which time the lacustrine sediments filled the available accommodation space in the caldera moat. Multiple analyses, including core sedimentology and stratigraphy, sediment density and rock magnetic properties, organic carbon content and carbon isotope ratios, C/N ratios, and pollen content reveal two glacial/interglacial cycles in the core (MIS 14 to MIS 10). This record includes glacial terminations V and VI and complete sections spanning interglacials MIS 13 and MIS 11. In the VC-3 record, both of these interglacials are relatively long compared with the intervening glacials (MIS 14 and MIS 12), and interglacial MIS 13 is significantly muted in amplitude compared with MIS 11. These features are similar to several other mid-Pleistocene records. The glacial terminations are quite abrupt in this record with notable changes in sedimentation, organic carbon content, C/N ratios and watershed vegetation type. Termination V is the largest climate change evident in this part of the middle Pleistocene. The glacial inceptions tend to be more gradual, on the order of a few thousand years.

INTRODUCTION

Paleoclimate records from lacustrine deposits in terrestrial settings typically span the Holocene and terminate in the late Pleistocene. In the southwest United States, such lake records have provided important information about the nature of the transition from the Last Glacial Maximum (LGM) into the Holocene (e.g., Enzel et al., 1992; Anderson, 1993; Allen and Anderson, 2000; Anderson et al., 2000; Castiglia and Fawcett, 2006;). In North America, only a few lacustrine records extend back in time beyond the late Pleistocene and are typically not sampled at a high resolution (Adam et al., 1989; Litwin et al., 1997; Davis, 1998). The longest nonlacustrine paleoclimate record from southwestern North America is from a vein calcite deposit in Devil's Hole, Nevada (Winograd et al., 1992).

Recent interest in the climate of the middle Pleistocene has focused on the long interglacial, Marine Isotope Stage 11 (MIS 11) ~ 400 ky ago, which is cited as a possible analog for future Holocene climates (Berger and Loutre, 1992; McManus et al., 2003). This interglacial is about 40 kyr in duration and may have been as warm as the Holocene with possibly elevated sea-levels relative to the Holocene (Droxler et al., 2003). Recent work in Antarctic ice cores documents significant differences in atmospheric CO_2 and climate change over the middle Pleistocene (EPICA, 2004; Siegenthaler, 2005) and a new oceanic benthic oxygen isotope stack representing global ice volume (Lisiecki and Raymo, 2005) shows similar prominent changes over the timespan from MIS 15 to MIS 9 (from ~600 ka to 360 ka). However, lacustrine and other terrestrial records spanning this critical interval of the middle Pleistocene are rare globally.

We present here preliminary results from a middle Pleistocene paleoclimate record from a lake sequence preserved in the eastern moat of the Valles Caldera, in northern New Mexico.

GEOLOGIC SETTING AND DRILLING DETAILS OF CORE VC-3

The 22 km diameter Valles caldera in the Jemez Mountains of northern New Mexico is an excellent example of a resurgent caldera (Smith and Bailey, 1968) that has a long and dynamic history of interaction between volcanic and hydrothermal processes (Goff and Gardner, 1994) and surficial processes. The caldera lies at the intersection of the Rio Grande rift and the Jemez volcanic lineament and contains a thick sequence of lacustrine sediments and hydromagmatic deposits that date from the inception of the caldera (ca. 1.23 Ma) to recent Pleistocene and Holocene bog deposits (Brunner Jass, 1999; Anderson et al., in review). Surficial exposures of lacustrine rocks occur on the uplifted flanks of the central resurgent dome and as eroded remnants within the encircling valleys (Smith et al., 1970; Goff et al., 2005a, b). Observations of these deposits show thick sequences of diatom-rich sediment (e.g., Valle San Antonio) and sediments with conifer macrofossils found on the early floor of the caldera.

The Valles caldera complex formed after the terminal pyroclastic eruption of a large shallow magma chamber, at 1.23 Ma (Phillips et al., in press). An almost immediate resurgence

within the caldera occurred (Smith et al., 1970; Phillips et al. in press), reflected today as Redondo Peak in the center of the caldera complex (Fig. 1). Field relationships show that a large lake formed in the caldera almost immediately (Goff et al., 2005a). This lake existed for an undetermined amount of time before the caldera wall was breached and the lake drained through San Diego Canyon, probably owing to the resurgence in the caldera. Over the next million years, a series of rhyolite domes erupted from ring fracture vents following the caldera collapse. Several lakes existed in the valleys after 0.8 Ma, when these postcaldera eruptive domes formed and temporarily blocked drainages to San Diego Canyon. A particularly long-lived lake formed in the Valle Grande during the middle Pleistocene when the South Mountain rhyolite dome erupted and blocked the drainage from the Valle Grande to San Diego canyon (Fig. 1). The age of the South Mountain rhyolite was determined as 521 ± 4 ka (Spell and Harrison, 1993) via Ar-Ar dating. As will be shown below, the age estimate of this eruption should probably be revised to 552 ka based on new Ar-Ar dates from a basal tephra in core VC-3 and from a geochemically similar tephra found outside the caldera, and geologic data reported here and in more detail in a companion paper (WoldeGabriel et al., 2007).

The focus of this work is on the sediments of the middle Pleistocene lake that formed after the eruption of the South Mountain rhyolite. Previous work on these deposits was based on cuttings from a deep water well drilled in the 1940s by the U.S. Geological Survey (USGS). This early drilling showed ~90 m of white- to olive-colored, clay-rich silt interpreted as lake bottom sediments, as well as sands and gravels (Conover et al., 1963) that locally contain pumice-rich layers. Sediments below the clay-rich zone consist of pumiceous sands and gravels (Conover et al., 1963) that extend to some undetermined depth. These water well logs also showed the presence of an artesian aquifer at ~86 to 90 m depth from the surface. An early pollen analysis on cuttings from the USGS water well showed pronounced cycles of wet to dry climates based on ratios of spruce and fir to spruce, fir, pine and oak (Sears and Clisby, 1952). Without any numerical age control, Sears and Clisby (1952) assumed that the uppermost lacustrine sediments were Holocene in age and the lower sediments aged progressively into the late Pleistocene. As we will show, the lacustrine sediments are middle Pleistocene in age, but this early work demonstrated the excellent potential for a long climate record from the Valle Grande.

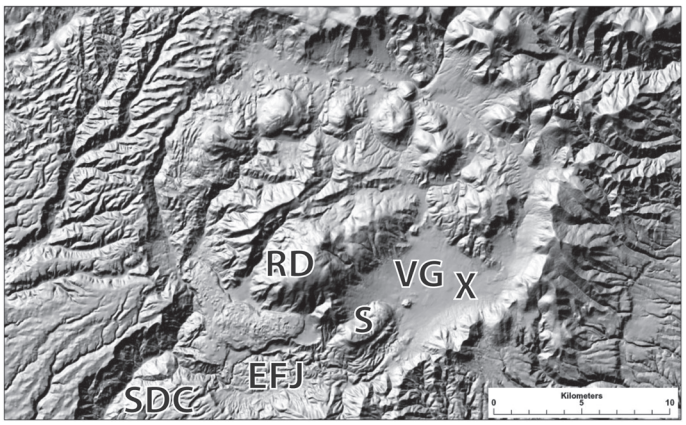

FIGURE 1. Location map of the Valles Caldera showing the Valle Grande (VG), location of hole VC-3 (X), the central resurgent dome (RD), San Diego Canyon (SDC), the East Fork of the Jemez River (EFJ) and the South Mountain Rhyolite dome (S).

New opportunities for scientific work in the Valles caldera opened in 2000 when the historic Baca Ranch, privately held for over 200 years, was sold to the Federal Government. The Valles Caldera Trust was created by the Valles Caldera Preservation Act of 2000 and was charged with managing the now public land, including continuing ranch operations as well as conducting numerous archeological, biological, and geological surveys. Interest in the geology and paleoclimate potential of sediments in the Valles Caldera led to the Valles Caldera Drilling Workshop in October 2003, sponsored by the Institute for Geophysics and Planetary Physics (IGPP) and members of Los Alamos National Lab EES-6, which was attended by 60 scientists (Goff and Heikoop, 2003). Two days of talks on Valles caldera geology and field trips into the caldera led to a partial consensus that the best target for a long lacustrine record would be in the Valle Grande.

METHODS

In May 2004, the deposits of the ancient Valle Grande lakes were cored with the DOSECC CS500 drill rig as the Global Lakes Drilling Project 5 (GLAD5). A single hole was drilled in the Valle Grande, VC-3, that achieved a total depth of 81.4 m and a ~75 m section of lacustrine mud, silts and gravels was recovered. Recovery of lacustrine mud and silt was close to 100%, while the recovery of fluvial gravels encountered at the top and bottom of the sequence was considerably less. Drilling was stopped at 81 m depth because of proximity to the artesian aquifer at ~86 m depth reported by the USGS (Conover et al., 1963), and because core recovery was very poor from 77-81 m depth. Despite this poor recovery at the base of the hole, we did recover a complete lower sequence of pumiceous sands and gravels that grade into a lacustrine silty mud sequence. At 5 m depth, the lacustrine deposits terminate at a nonconformity, which is overlain by coarse Holocene fluvial gravels and meadow deposits.

Core VC-3 was transported to the National Lacustrine Core Facility (LacCore) at the University of Minnesota in June 2004. Prior to splitting, the whole round-core sections were logged with the LacCore Geotek multisensor core logging system and data were acquired at 1 cm intervals for magnetic susceptibility, gamma ray densitometry, electrical resistivity, and P-wave velocity. Sediment density was measured by calibrated gamma-ray attenuation giving a field or wet sediment measurement. Magnetic susceptibility was measured by a Bartington loop sensor that integrates the field measurement over a 10 cm volume. After the core was split, the archive half was imaged at a resolution of 10 pixels/mm, wrapped and moved to cold storage.

During the initial core description, we identified 67 sedimentary units following procedures outlined in Schnurrenberger et al. (2001). Macroscopic observations were supplemented by microscopic smear slide estimates of mineralogy and other sedimen-

tary components, spaced approximately every 50 cm down the length of the core. Two samples were submitted for XRD analysis, which showed the presence of siderite in parts of the core. A series of U-channels were taken from the core for analysis, which were subsequently x-rayed at the University of New Mexico Hospital radiology department.

Samples were taken for several types of analyses, including paleomagnetic and rock magnetic analyses, sediment geochemistry, pollen analysis, organic carbon, organic carbon stable isotopes, and C/N ratios. Sample spacing ranges from 20 cm for rock magnetic work to 0.5 to 1 m for pollen and organic carbon analyses and results are reported for oven-dry weights. Sedimentologic and stratigraphic analyses were conducted by direct core observations as described above and work with digital image files of the core. Organic carbon content and organic carbon isotopes were measured on an elemental analyzer and an isotope ratio mass spectrometer. The presence of siderite, an iron carbonate, in multiple levels of the core added a complication for these measurements, in that the siderite carbon content would be included in total organic carbon measurements. It would also skew the isotopic analyses of organic carbon. Thus, samples for organic carbon analyses were pretreated twice with concentrated 6N HCL at 60°C to remove any siderite grains from the material. Pollen samples were treated following standard protocols at the Laboratory of Paleoecology (Northern Arizona University) for isolating pollen grains.

RESULTS

Introduction and age

Our preliminary analyses show considerable downcore variability in sedimentary facies, magnetic susceptibility, and gamma ray density (Fig. 2). The basal section of the core consists of indurated rhyolitic sands and gravels interbedded with indurated muds. We initially hypothesized that these gravels would be associated with the eruption of the South Mountain Rhyolite as the eruption of this rhyolite dome dammed the drainage from the Valle Grande. This would constrain the base of the core to 521 ± 4 ka, based on published ^{40}Ar-^{39}Ar dates from the South Mountain Rhyolite (Spell and Harrison, 1993). To confirm this, fresh, glassy material from a thin tephra at ~75 m depth and pumice from gravel just below the tephra were submitted to the New Mexico Geochronology Research Laboratory (Socorro) for ^{40}Ar-^{39}Ar dating. These samples yielded dates of 550 ± 20 ka for single crystal analysis of sanidines and 552 ± 3 ka for multiple crystal analysis. The presence of abundant sanidine crystals in the tephra and in the pumice layers submitted allowed for good precision and accuracy given the relatively small sizes of the samples submitted. These dates confirm that the base of the core recovered is indeed middle Pleistocene in age but they also show that the early deep lake deposits are slightly older than the previously published ^{40}Ar-^{39}Ar dates for the South Mountain rhyolite. Trace element analyses conducted on the tephra were found to precisely match the trace element geochemistry of the South Mountain rhyolite, confirming the origin of the tephra. The tephra geochemistry is demonstrably different from other rhyolite domes in the caldera (WoldeGabriel, et al., 2007). In addition, a tephra found in a fluvial terrace deposit in the Santo Domingo basin outside of the caldera has an ^{40}Ar-^{39}Ar date of 551 ± 1 ka (Smith et al., 2001), further substantiating the VC-3 tephra data. No other tephras are found in the Valle Grande core above the basal tephra and in fact, no evidence of a nearby volcanic eruption can be found in the core. Recent geologic mapping shows no other rhyolite units that could have served as a hydrologic dam to the Valle Grande prior to the eruption of the South Mountain rhyolite (Goff et al., 2005a). A plausible way to resolve these somewhat disparate data sets is to argue that the published ^{40}Ar-^{39}Ar date for the South Mountain rhyolite (Spell and Harrison, 1993) is too young and that in fact it should be ~552 ka. W. McIntosh (New Mexico geochronology laboratory) is redating the four flow lobes of the South Mountain rhyolite (Goff et al., 2005a) and this should ultimately resolve the issue.

VC-3 sedimentology and stratigraphy

Deposits above the basal gravels and sands grade upwards into muddy silts and then silty muds that range from finely laminated to moderately bioturbated in character (Fig. 2). Much of the lacustrine mud sequence is enriched in diatoms, and the density and diversity of diatom taxa are variable down the length of the core. In the lower part of the lacustrine sequence, several turbidites (up to a meter thick) and decimeter-thick gravels interrupt the laminated mud sequences. The silty muds contain well-preserved mm-scale laminations from ~76 m depth to ~52 m depth. From 52 to 48 m depth, sediments are thickly laminated to thinly bedded with little bioturbation evident. At 48 m depth, a series of facies changes (from laminated to structureless) continue until

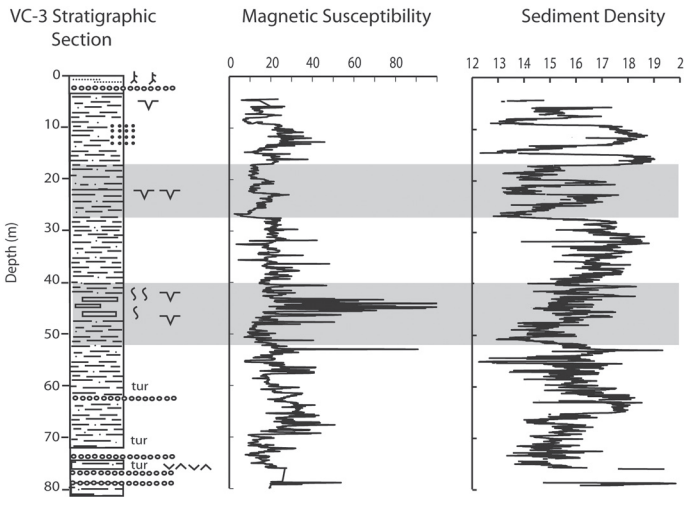

FIGURE 2. Simplified stratigraphic section for core VC-3. Standard stratigraphic symbols are used, except for tur = turbidite, rectangles at ~45 m depth represent blocky facies, circles represent gravels. Also shown are bulk magnetic susceptibility (cgs x 10^{-6}) and bulk sediment density (g/cm^3). Gray bars represent depths of interpreted interglacial climate periods as discussed in the text.

42 m depth. Over this interval, multiple cm-scale mudcracks are evident and bioturbation is common. Decimeter-scale blocks of color change correlate strongly with magnetic susceptibility where darker sediments have much higher magnetic susceptibilities. The rapid facies changes within this interval and the multiple mudcracks present indicate relatively shallow water conditions with episodic lake drying events. From 42 to 39 m depth, the sediments are again thickly laminated to thinly bedded with no mudcracks evident. At 39 m depth, sediments grade back to well-laminated silty mudstones (mm-scale laminations again) until 27 m depth. From 27 to 17 m depth, sediments are again thickly laminated to thinly bedded, and a prominent meter-deep mudcrack is developed at 23 m depth. From 17 m depth to 5 m depth, sedimentary structures are variable with well-laminated silty mudstones alternating with thickly laminated to thinly bedded silty mudstones. In this last depth interval, thin sandy lenses occur (from ~13 to 10 m depth) and occasional rhyolitic dropstones are found (which are especially evident in x-radiographs of the core). The uppermost lacustrine mud to gravel transition at 5 m depth probably represents an unconformity from mid-Pleistocene age to Holocene gravels and soil developed in fluvial overbank/meadow deposits.

VC-3 magnetic susceptibility variations

Magnetic susceptibility (MS) results show considerable variability down the length of the core with values as low as 10 x 10^{-6} cgs and as high as 100 x 10^{-6} cgs (Fig. 2). The bulk magnetic susceptibility measurements broadly correlate with the changes in sedimentary facies noted above. From 76 to 53 m depth, MS values are highly variable and appear to correlate with changing detrital input to the lake, including gravels, turbidites and quiet water laminations. At 53 m depth, MS values decline to very low values until 48 m depth, where values increase sharply. The highest MS values in the core occur between 48 m depth and 42 m depth, and rock magnetic tests indicate that the primary magnetic mineral present is the sulfide greigite (Fe_3S_4) (Donohoo-Hurley et al., 2007). MS values are less variable from 42 to 27 m depth; at 27 m depth MS values drop considerably. Above 17 m depth, MS values increase again, with one prominent lower value region at about 15 m depth (Fig. 2). Further details of the rock magnetic, as well as paleomagnetic, properties of the core are presented by Donohoo-Hurley et al. (2007).

VC-3 sediment density

The sediment field (wet) bulk density of core VC-3 is highly variable with values ranging from a low of 1.3 g/cc to a high of 1.8 g/cc. The downcore density trends broadly match those of magnetic susceptibility with some important differences (Fig. 2). Sediment density is variable from 76 to 53 m depth where it decreases dramatically. From 53 to 42 m depth, density gradually increases and there is no good correlation with the high magnetic susceptibility values over this interval. Density increases from 40 to 27 m depth, at which point it decreases dramatically to some of the lowest values in the core. From 27 to 17 m, sediment density is predominantly low, although short intervals of higher density do occur within this range (Fig. 2). At 17 m depth, density increases abruptly to some of the highest values in the core, and remains high to the top of the core, except for two prominent lows at 15 and 9 m depth.

VC-3 organic carbon and carbon isotopes

Total organic carbon (TOC) and organic carbon isotopes ($\delta^{13}C$) show variations down the length of the core that correlate very well with changes in sedimentary facies, MS, and sediment density. Low TOC values characterize the deepest part of the core from 76 to 53 m depth, where values range from ~0.3% to 1.2%. Organic carbon isotopic values ($\delta^{13}C$) over this interval are light and vary from -25 to -27‰ (Fig. 3). A sharp increase in TOC at 53 m depth correlates with the prominent facies changes noted above. Here, TOC values are relatively high (up to 3%) and $\delta^{13}C$ values are heavier, ranging from -22 to -24‰. From 48 to 42 m depth, TOC values decline to less than 1% and organic carbon $\delta^{13}C$ values become significantly lighter (-27‰). From 42 to 39 m depth, TOC values are higher (up to 3%) and organic carbon $\delta^{13}C$ values are heavier (-22 to -24‰). At ~39 m depth, TOC values decline dramatically and remain low (less than 1%) until 27m depth. Organic carbon $\delta^{13}C$ values are also relatively light (-26‰) over this interval. A sharp increase in TOC is noted at 27 m depth where values rise to over 5%. The highest TOC values in the core occur between 27 and 17 m depth, although the values vary considerably. These high TOC values correlate with low values of MS and sediment density. Over this same interval, $\delta^{13}C$ values are also variable, but reach their heaviest values in the core of -19 to -22‰. At 17 m depth, TOC falls and $\delta^{13}C$ values decrease, in conjunction with the abrupt increases noted in MS and sediment density. A local high in organic carbon from 15 to 13 m depth is matched by an increase in $\delta^{13}C$ values.

C/N ratios track the relative inputs of terrestrial organic matter vs. lacustrine algal organic matter in the lake, with lower values

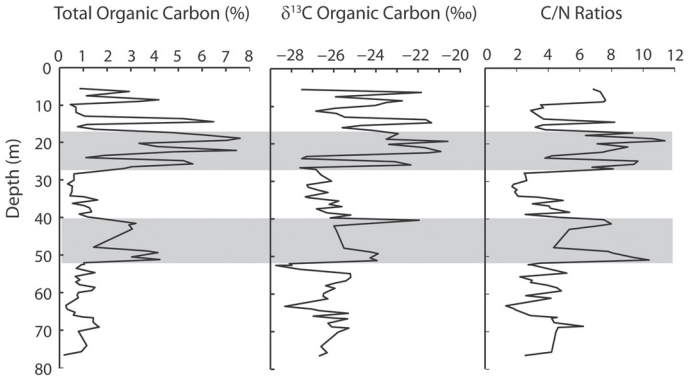

FIGURE 3. Total organic carbon in the siderite-free fraction of core VC-3 expressed as a percentage of the total weight percent. Organic carbon isotopes (expressed as ‰ relative to PDB standard) and C/N ratios in the siderite free fraction. Gray bars represent depths of interpreted interglacial climate periods as discussed in the text.

consistent with greater algal matter (Meyers and Ishiwatari, 1995). The VC-3 C/N ratios follow the general trend of TOC content in the core with higher values (6 to 8) when organic carbon values are high and lower values (2 to 4) when organic carbon values are lower (Fig. 3). The highest C/N ratios are found over two intervals from 52 to 39 m depth and from 27 to 17 m depth, times when TOC is highest and $\delta^{13}C$ values are the most enriched.

VC-3 pollen

Pollen analysis was initiated at widely spaced intervals to provide a paleovegetation framework for the core, and to compare with an earlier pollen diagram (Sears and Clisby 1952). Our initial sampling interval varied from 0.2 to 5.9 m, with an average of 1.8 m. Samples from the bottom 10 m of the core (Fig. 4) are dominated by conifers, primarily spruce (*Picea*) and pine (*Pinus*). Such high percentages (up to 40% for each) are presently unknown in the modern pollen rain of the region (Brunner Jass, 1999; Anderson et al. 2004), and suggest dense boreal conifer forest vegetation. Sediments from ca. 65 m to ca. 34 m depths are dominated by pine and spruce, but this time with sagebrush (*Artemisia*) and other shrubs (sunflower [Asteraceae] and goosefoot [Chenopodiaceae-*Amaranthus*] families, and grass (Poaceae), among others (Fig. 4). These pollen samples are most similar to latest Pleistocene spectra from analogous elevations in the southern Rocky Mountains (Toney and Anderson, 2006; Anderson et al. 2004) and southern Colorado Plateau (Anderson et al., 2000). Pollen samples above 34 m show a reduction in spruce, but an increase in mixed conifer elements (fir [*Abies*], Douglas-fir [*Pseudotsuga menziesii*]), as well as hardwoods (oak and birch [*Betula*]). These pollen spectra are consistent with modern pollen assemblages within the caldera (Brunner Jass, 1999), and suggest interglacial conditions. Highest oak and ragweed (*Ambrosia*) pollen percentages occur from 27 to 17 m depth, perhaps suggesting "thermal maximum-like" conditions for this interval. A final reversal to more glacial-like pollen spectra lies at about 17 m depth (Fig. 4). Our results are broadly consistent with Sears and Clisby (1952), who studied a 65 m-thick core ~100 m from the VC-3 hole, and proposed periods of wet and dry conditions based on specific pollen ratios. Wetter conditions were suggested for core segments below about 57 m, from about 42 to 27 m, and above 17 m in the core. Drier conditions were suggested for core sections from 57 to 42 m and 27 to 17 m.

DISCUSSION

Many of the parameters measured in VC-3 show dramatic changes that are broadly correlative and consistent with colder and wetter periods vs. warmer and drier periods. We interpret the broad organic carbon, C/N ratio, pollen, and sedimentologic trends to indicate three cold and wetter intervals (from 76 to 53 m; from 38 to 27 m; and from 17 to 5 m depth) and two warmer and drier intervals (from 53 to 38 m and from 27 to 17 m depth) in VC-3. The wet vs. dry periods we interpret here are very similar to those reported by Sears and Clisby (1952), and these drier periods correspond to our preliminary reconstructions of interglacial "thermal maximum" periods. The TOC shows the most pronounced differences between warm and cold intervals with

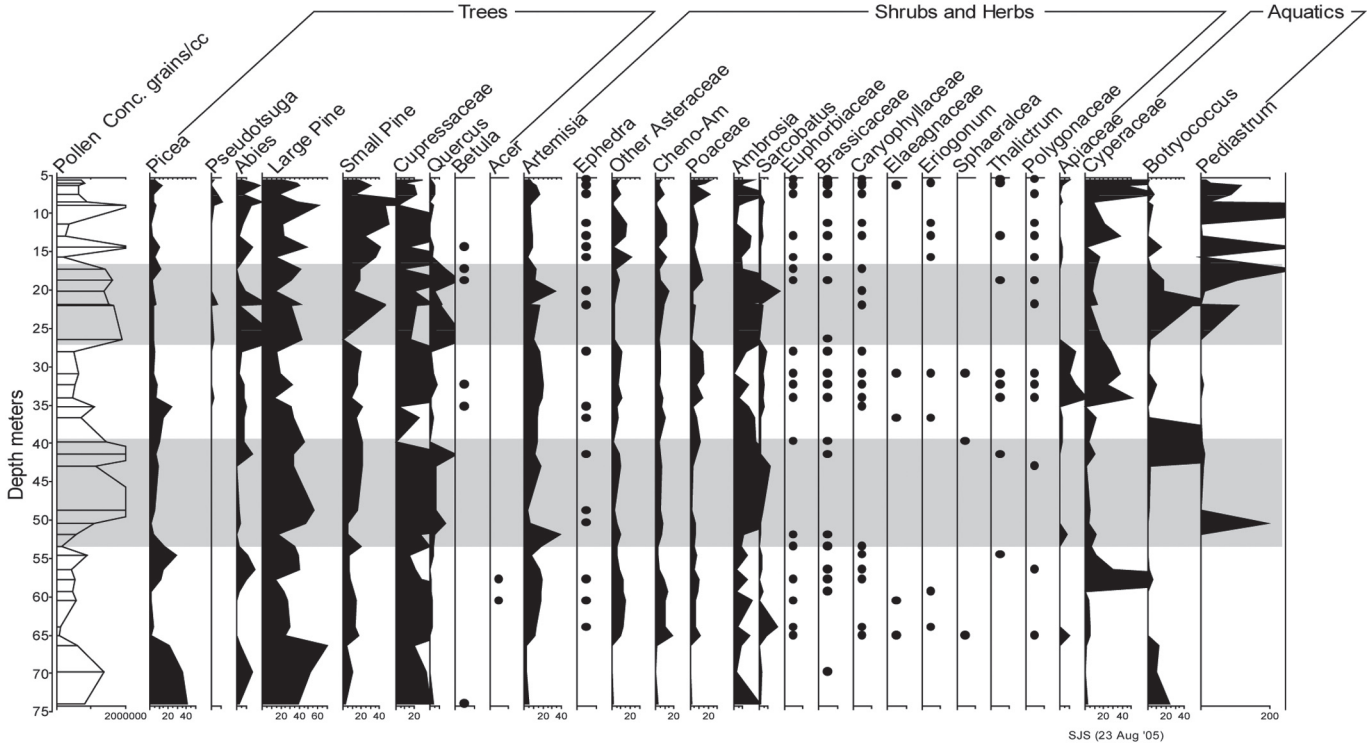

FIGURE 4. Summary pollen diagram for core VC-3. Silhouette is 10X actual amount. Dots denote < 1% of the pollen sum.

cold intervals being correlated with diminished lacustrine productivity. Bischoff et al. (1997) reported similar results in TOC for glacial vs. interglacial conditions in a deep core from Owens Lake, CA.

In core VC-3, interglacial intervals are characterized by higher organic carbon content driven primarily by increased lacustrine productivity. The organic C/N ratios are consistent with this pattern, with elevated ratios occurring during times of increased organic carbon, and lower ratios occurring during times of decreased organic carbon, interpreted as glacial periods. Higher C/N ratios are consistent with a greater input of terrestrial organic matter into the lake (Meyers and Ishiwatari, 1995), although even at their highest values (6 to 8), the VC-3 C/N ratios are still dominated by algal lacustrine sources. Organic carbon $\delta^{13}C$ values are also broadly consistent with these interpretations. During interglacial periods, $\delta^{13}C$ values are heavier, which is consistent with enhanced productivity and possibly a switch to more C_4 plants in the watershed (especially for the 27 to 17 m depth interval). Magnetic susceptibility and sediment density trends are also consistent with these interpreted glacial-interglacial variations. During interglacial periods, the lake biological productivity is greatly enhanced with higher diatom productivity. As a result, the terrigenous input to the lake is diluted by higher biogenic silica amounts, as seen in the greatly reduced sediment densities and magnetic susceptibilities (especially between 27 and 17 m depth, Fig. 3). We do not have direct biogenic silica measurements in core VC-3; however, our smear slide analysis shows a higher abundance of diatom frustules relative to terrigenous material during the interglacial periods than during the glacial periods.

Glacial periods in VC-3 are characterized by low TOC values and lighter $\delta^{13}C$ values, reflecting lower aquatic biological productivity and a dominantly algal organic matter source. The very low C/N ratios are consistent with these interpretations. During glacial periods when the lake biological productivity is reduced, the sediment has a relatively larger terrigenous source component and both magnetic susceptibilities and sediment densities are relatively high.

The sedimentary facies present also show a strong correlation with interpreted glacial and interglacial periods. Glacial periods in the lake are characterized by well-laminated silty mudstones probably indicative of a relatively deep lake and therefore a wetter climate. Interglacial periods are characterized by less well-laminated silty mudstones, more bioturbation, and numerous mudcracks. The presence of mudcracks between 48 and 42 m depth and again between 27 and 17 m depth indicate rapid water level changes in an overall shallower lake. The prominent meter-deep mudcrack at 23 m depth with an oxidized upper decimeter indicates a complete desiccation of the lake. Following this event, the lake refilled and resumed depositing lacustrine silty mudstones. During both interglacial intervals, these sedimentary features are consistent with a shallower lake and a drier climate than the glacial periods.

These wetter (glacial) and drier (interglacial) climatic interpretations are consistent with the magnitude of hydroclimatic changes in the Southwest from the Last Glacial Maximum (LGM) to the Holocene. During the LGM, effective precipitation increased in the Southwest as shown by the presence of numerous large and small pluvial lakes (Lake Lahontan, Nevada; Lake Bonneville, Utah; Lake Estancia, New Mexico; and Lake Palomas, Mexico; Smith and Street-Perrott, 1983, Allen, 2005, Castiglia and Fawcett, 2006). These lakes formed during the glacial period because of colder temperatures and reduced evaporation rates, and because the Laurentide Ice Sheet in northern North America deflected the polar jet stream south, bringing more winter storms to the Southwest (COHMAP, 1988). In contrast, the interglacial Holocene in the Southwest was warmer and drier. The VC-3 record shows a similar pattern in hydroclimatic variability between glacials and interglacials in the middle Pleistocene, with distinctly wetter glacial periods and drier interglacials. We therefore interpret similar changes in atmospheric temperatures and circulation patterns for the middle Pleistocene, with pre-Laurentide ice sheets over northern North America deflecting the polar jet stream to the south.

VC-3 core chronology

A detailed chronology for the VC-3 core has been a challenge to establish because it is middle Pleistocene in age and all autochthonous organic material is radiocarbon dead. The previously discussed Ar-Ar date of 552 ± 3 ka from a basal tephra and from an underlying pumiceous deposit at 75.6 m depth constrains the core to the middle Pleistocene. We interpret the abrupt and dramatic increases in total organic carbon (and correlative changes in other core parameters such as C/N ratios, sediment density. and magnetic susceptibility) at 51.5 m depth and again at 27 m depth as clearly representing glacial terminations (Fig. 2). We correlate these dramatic changes in multiple proxies with Glacial Terminations VI and V respectively, as these are the first glacial terminations following the basal 552 ka date. We correlate these VC-3 terminations in time with an updated deep-sea global ice-volume curve (Lisiecki and Raymo, 2005), which provides orbitally-tuned dates of 533 ka and 424 ka. An alternative correlation would be with the Devil's Hole, Nevada vein calcite record; however, for the time period of interest (552 ka to ~400 ka), the error in the Devil's Hole U-series age dates is large enough to include the orbitally derived dates of the SPECMAP curve (Winograd et al., 1992). Additionally, we can also define two glacial onsets in core VC-3 based on total organic carbon content and other parameters. The MIS 13 to MIS 12 transition occurs at ~39.5 m depth (ca. 488 ka; Lisiecki and Raymo, 2005) and the MIS 11 to MIS 10 transition occurs at 17 m depth (Fig. 5) (ca. 395 ka, Lisiecki and Raymo, 2005; Winograd et al., 1992). Our primary age assignments are based on the sharp and well-defined glacial terminations.

An independent check on these age assignments is provided by preliminary paleomagnetic work on core VC-3, as discussed in greater detail in Donohoo-Hurley et al. (2007). Progressive demagnetization has identified two short-lived magnetic field "features" or excursions at 17.25 m and at 52.3 m depth in the core, where negative inclination magnetizations have been either well resolved or implied by demagnetization trajectories. We tentatively correlate these negative inclination features with globally recognized events 11α (406 ka) and 14α (536 ka) (Lund et al.,

2001). The approximate dates and depths of these magnetic field events match well with the dates and depths of the glacial terminations, supporting this age model. We would predict the presence of another geomagnetic field event somewhere in the 45 to 50 m depth interval, the globally recognized Calabrian Ridge II event (Singer et al., 2002). This interval of the core, however, is marked by very high magnetic susceptibility. Preliminary rock magnetic data show that this interval is largely dominated by greigite (Fe_3S_4), which is typically an authigenic phase in such sediments. The likelihood of the preservation of a primary remanence over this interval is low (Roberts et al., 1996), thus explaining why the Calabrian Ridge II event is not observed in this record. Good correlations of the magnitudes and durations of interglacials MIS 13 and 11 in VC-3 (Fig. 5) with those in other records including SPECMAP (Lisiecki and Raymo, 2005), Antarctica (Siegenthaler et al., 2005), and Lake Baikal (Prokopenko et al., 2002) strongly support this age model.

Above ~53 m depth, a linear regression through the age model data indicates an average sedimentation rate of ~0.25 mm/yr (Fig. 6). This slow sedimentation rate is consistent with the very small, forested catchment of the lake basin and a relatively deep lake. Interglacial periods appear to have higher sedimentation rates (~0.35 mm/yr) and glacial periods lower rates (0.19 mm/yr) and we account for this in our age-depth model. We hypothesize that the higher sedimentation rates during the interglacials are the result of greater lake productivity and greater biogenic silica input to the lake sediments. The lower part of the core is characterized by several turbidites (up to 1 m thick), gravels, and thickly bedded silty muds. These rapid sedimentation events are common in the initial stages of caldera infilling (Bacon et al., 2002; Larsen and Smith, 1999) and in VC-3 these features are consistent with the much higher sedimentation rates for the lower part of the core, as implied by the age model.

Characteristics of individual glacial and interglacial stages in VC-3

MIS 14: The deepest part of core VC-3, from 76 to 53 m depth, contains abundant evidence for a cold, wet climate. TOC, and C/N ratios are low and $\delta^{13}C$ values are negative indicating low organic productivity with a primarily algal source. Pollen trends indicate a dense spruce forest in the watershed in the lowest 10 m, and a pollen spectrum similar to late Pleistocene spectra from the southern Rocky Mountains. Sediments in this part of the core are well laminated, suggesting a relatively deep lake and a wetter climate.

MIS 13: The abrupt increase in TOC at 53 m depth marks glacial termination VI and a transition from cold, wet conditions to warmer, drier conditions in the Valle Grande watershed. Pollen samples from this interval show an increase in pine, oak, juniper, and warm desert shrubs (e.g., ragwood [*Ambrosia*)] and greasewood [*Sarcobatus*]). The first three pollen types are consistent with modern pollen assemblages within the caldera, and support the interglacial interpretation, while the last two are probably from long-distance sources. Our initial sampling interval in VC-3, while relatively coarse, shows that TOC is quite variable during MIS 13, with two "warm" (high TOC) episodes at the beginning and end of the stage with a prominent cold interval

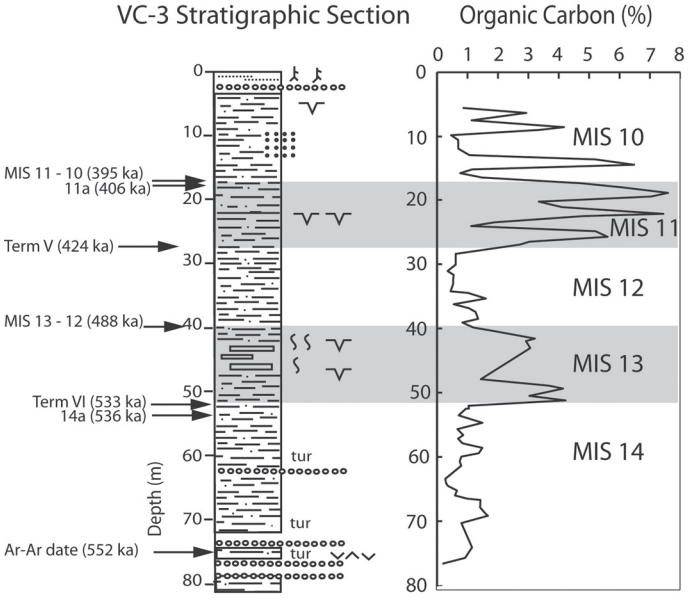

FIGURE 5. Age model for core VC-3. Dates are based on Ar-Ar analysis, correlations of abrupt TOC increases with glacial terminations VI and V, correlations of paleomagnetic field events with globally recognized events (14a and 11a) and correlations of TOC decreases with glacial onsets (timing from Lisiecki and Raymo, 2005). Gray bars represent interpreted interglacial stages (MIS 13 and MIS 11) while white bars represent glacial stages (MIS 14, MIS 12 and MIS 10) as labeled.

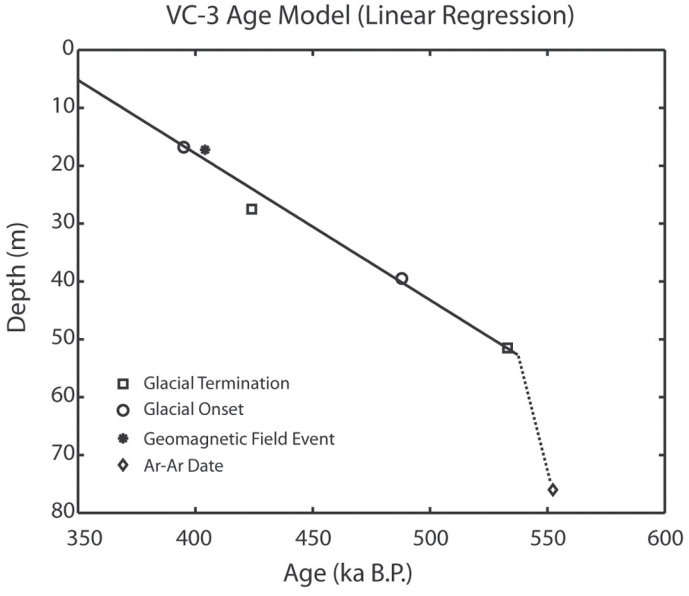

FIGURE 6. Linear regression of age-depth tie points in core VC-3. Symbols in figure represent different age tie-points as labeled. The linear regression is from 5 to 53 m depth. Below 53 m depth, sedimentation rates in the core are significantly higher, representing the initial infilling of the lake as discussed in the text.

in the middle (48 to 42 m depth; Fig. 3) – perhaps analogous to intra-Eemian cooling noted elsewhere (e.g., Adams et al., 1999; Karabanov et al., 2000). The same warm-cold-warm pattern is repeated in the C/N ratios, $\delta^{13}C$ values, pollen and sedimentology. The TOC values for MIS 13, while substantially higher than the glacial periods around it, are lower than for MIS 11 higher in the core (Fig. 3), suggesting that this is a muted interglacial relative to MIS 11. Notably, atmospheric CO_2 levels are lower during MIS 13 than MIS 11 (Siegenthaler et al., 2005) and a prominent interglacial cold stage with low pCO_2 in the middle of MIS 13 is matched by the interglacial cold period in the VC-3 record. The SPECMAP ice volume curve (Lisiecki and Raymo, 2005) also shows the same cold interglacial phase between two warmer intervals during MIS 13.

MIS 12: From ~39 m to 27 m depth, TOC, C/N ratios, and $\delta^{13}C$ values show a progressive decrease, indicating progressively colder glacial conditions. Based on TOC values, the MIS 12 glacial maximum occurs at ~30 m depth. Sediments are well laminated, again indicating a relatively deep lake and a wetter climate. Pollen assemblages from this depth are again conifer dominated, showing an increase in spruce consistent with a cold, wet glacial period.

MIS 11: At 27 m depth, another abrupt increase in TOC and several other parameters marks glacial termination V. In global records, termination V is the largest amplitude glacial-interglacial transition over the last million years (Lisiecki and Raymo, 2005; EPICA members, 2004; Siegenthaler et al., 2005) and this termination is the largest climate change event in core VC-3. MIS 11 is characterized by the highest TOC values in the core, high C/N ratios and the highest oak and ragweed (*Ambrosia*) pollen percentages, suggesting "thermal maximum-like" conditions. In VC-3, there are no prominent intraglacial cold periods in MIS 11; however, TOC is variable throughout this period, possibly reflecting periodic drying of the lake and oxidation of preexisting organic matter. The coincidence of the prominent meter-deep mudcrack with low TOC values at 23 m depth supports this interpretation. The apparent duration of interglacial MIS 11 is ~ 30 kyr in this record.

MIS 10: The first 6-7 kyr of MIS 10 (17 m to 15 m depth) are cold as shown by pollen, TOC, very high bulk density values, and other core parameters. At 15m depth (~388 ka), TOC sharply increases (values as high as 5%) as do several other parameters (except pollen where no strong warm signal is present). This apparent warm period (interstadial) lasts for ~ 5 to 6 kyr and is followed by a more pronounced glacial period. This early MIS 10 warm event is well defined in this record; however, in less well-resolved records, it could be interpreted as part of MIS 11. If this warm interval was included in MIS 11, the entire length of MIS 11 would be ~42 kyr. We do not include this warm interval in the interglacial because the glacial onset at 17 m depth is so pronounced in all of the core parameters, and pollen indicators remain cold over this interval. Sediment grain size is coarser during this glacial than previous glacials, but at these shallow depths in the core, the lake had largely filled in its accommodation space, resulting in a geomorphically shallower lake than the wetter climate conditions would suggest.

CONCLUSIONS

Core VC-3 spans a considerable interval of the mid-Pleistocene and records two full glacial cycles (MIS 14 to MIS 10). Glacial periods in the core are generally characterized by low TOC, more negative $\delta^{13}C$ values, lower C/N ratios, higher spruce pollen, higher bulk density, higher magnetic susceptibility and generally well-laminated silty mudstones. Interglacial periods are generally characterized by high TOC values, more positive $\delta^{13}C$ values, higher C/N ratios, higher pine, oak and juniper pollen, lower bulk density, lower magnetic susceptibility (except high MS values in middle of MIS 13 due to the mineral greigite) and less well-laminated sediments with mudcracks and more bioturbation present. Glacial terminations are abrupt in the core, and termination V (MIS 12 to MIS 11) is the largest climate change recorded in the core. Interglacial MIS 13 is more muted than MIS 11, consistent with other long Pleistocene records including Devil's Hole, Lake Baikal, Dome C ice core, Antarctica, and the marine deep-sea oxygen isotope stack.

ACKNOWLEDGMENTS

Funding for this work was provided by the USGS Western Mountain initiative (Allen), LANL IGPP (Heikoop, Fawcett, Goff) and the NSF Paleoclimate Program (Fawcett, Geissman).

Core VC-3 is archived at and assistance was provided by LRC/LacCore, University of Minnesota. We gratefully acknowledge the Valles Caldera Trust and Bob Parmenter (Head Scientist) for permission to drill in the Valle Grande. This manuscript benefited greatly from reviews by Bruce Allen and Kirsten Menking.

REFERENCES

Adam, D.P., Sarna-Wojcicki, A.M., Rieck, H.J., Bradbury, J.P., Dean, W.E., and Forester, R.M., 1989, Tulelake, California: the last 3 million years: Palaeogeography, Palaeoclimatology, Palaeoecology, v. 72, p. 89-103.

Adams, J., Maslin, M., and Thomas, E., 1999, Sudden climate transitions during the Quaternary: Progress in Physical Geography v. 23, p. 1-36.

Allen, B.D., 2005, Ice Age lakes in New Mexico: New Mexico Museum of Natural History and Science, Bulletin 28, p.107-114.

Allen, B.D., and Anderson, R.Y., 2000, A continuous, high-resolution record of late Pleistocene climate variability from the Estancia Basin, New Mexico: Geological Society of America Bulletin, v. 112, p. 1444-1458.

Anderson, R.S., 1993, A 35,000 year vegetation and climate history from Potato Lake, Mogollon Rim, Arizona: Quaternary Research, v. 40, p. 351-359.

Anderson, R.S., Betancourt, J.L., Mead, J.I., Hevly, R.H., and Adam, D.P., 2000, Middle and Late Wisconsin paleobotanic and paleoclimatic records from the southern Colorado Plateau, USA: Palaeogeography, Palaeoclimatology, Palaeoecology, v. 155, p. 31-57.

Anderson, R.S., Allen, C.D., Toney, J.L., Jass, R.B., and Bair, A.N., 2004, Holocene vegetation and forest fire regimes in subalpine and mixed conifer forests, southern Colorado and northern New Mexico, USA: Pollen, v. 14, p. 220.

Bacon, C.R., Gardner, J.V., Mayer, L.A., Buktenica, M.W., Dartnell, P., Ramsey, D.W., and Robinson, J.E., 2002, Morphology, volcanism and mass wasting in Crater Lake, Oregon: Geological Society of America Bulletin, v. 114, p. 675-692.

Berger, A., and Loutre, M.F., 2002, An exceptionally long interglacial ahead?: Science, v. 297, p. 1287-1288.

Bischoff, J.L., Fitts, J.P., and Fitzpatrick, J.A., 1997, Responses of sediment geochemistry to climate change in Owens Lake sediment: an 800-k.y. record of saline/fresh cycles in core OL-92: Geological Society of America, Special

Paper 317, p. 37-47.
Brunner Jass, R.M., 1999, Fire occurrence and paleoecology at Alamo Bog and Chihuahueños Bog, Jemez Mountains, New Mexico, USA [M.S. Thesis]: Flagstaff, Northern Arizona University.
Castiglia, P.J., and Fawcett, P.J., 2006, Large Holocene lakes and climate change in the Chihuahuan Desert: Geology, v. 34, p. 113-116.
COHMAP Members, 1988, Climatic changes of the last 18,000 years: observations and model simulations: Science, v. 241, p. 1043-1052.
Conover, C.S., Theis, C.V., and Griggs, R.L., 1963, Geology and hydrology of Valle Grande and Valle Toledo, Sandoval County, New Mexico: U.S. Geological Survey, Water-Supply Paper 1619-Y, 37 p.
Davis, O.K., 1998, Palynological evidence for vegetation cycles in a 1.5 million year pollen record from the Great Salt Lake, Utah, USA: Palaeogeography, Palaeoclimatology, Palaeoecology, v. 138, p. 175-185.
Donohoo-Hurley, L., Geissman, J.W., Fawcett, P.J., Wawrzyniec, T., and Goff, F., 2007, A 200 kyr lacustrine record from the Valles Caldera: insight from environmental magnetism and paleomagnetism: New Mexico Geological Society, 58th Field Conference, Guidebook, p. 424-432.
Droxler, A.W., Poore, R.Z., and Burckle, L.H., eds, 2003, Earth's climate and orbital eccentricity: the marine isotope stage 11 question: American Geophysical Union. Geophysical Monograph 137, 240 p.
Enzel, Y., Brown, W.J., Anderson, R.Y., McFadden, L.D., and Wells, S.G., 1992, Short-duration Holocene lakes in the Mojave River drainage basin, southern California: Quaternary Research, v. 38, p. 60-73.
EPICA Community Members, 2004, Eight glacial cycles from an Antarctic ice core: Nature, v. 429, p. 623-628.
Goff, F., and Gardner, J.N., 1994. Evolution of a mineralized geothermal system, Valles caldera, New Mexico, Economic Geology, v. 89, p. 1803-1832.
Goff, F., and Heikoop, J.M., 2003, Workshop weighs climate change studies at Valles caldera: EOS, Transactions of the American Geophysical Union, v. 84, no. 50, p. 563.
Goff, F., Gardner, J.N., Reneau, S.L., and Goff, C.J., 2005a, Preliminary geologic map of the Redondo Peak quadrangle, Sandoval County, New Mexico: New Mexico Bureau of Geology and Mineral Resources, Open-file Geologic Map OF-GM-111, scale 1:24,000.
Goff, F., Reneau, S.L, Lynch, S., Goff, C.J., Gardner, J.N., Drakos, P. and Katzman, D., 2005b, Preliminary geologic map of the Bland quadrangle, Los Alamos and Sandoval Counties, New Mexico: New Mexico Bureau of Geology and Mineral Resources, Open-file Geologic Map OF-GM-112, scale 1:24,000.
Karabanov, E.B., Prokopenko, A.A., Williams, D.F., and Khursevich, G.K., 2000, Evidence for mid-Eemian cooling in continental climatic record from Lake Baikal: Journal of Paleolimnology, v. 23, p. 365-371.
Larsen, D., and Smith, G.A., 1999, Sublacustrine-fan deposition in the Oligocene Creede Formation, Colorado, U.S.A.: Journal of Sedimentary Research, v. 69, p. 675-689.
Lisiecki, L.E., and Raymo, M.E., 2005, A Pliocene-Pleistocene stack of 57 globally distributed benthic delta ^{18}O records: Paleoceanography, v. 20, PA1003 doi:10.1029/2004PA001071
Litwin, R.J., Adam, D.P., Frederiksen, N.O., and Woolfenden, W.B., 1997, An 800,000-year pollen record from Owens Lake, California: preliminary analyses: Geological Society of America, Special Paper 317. p. 127-142.
Lund, S.P., Williams, T., Acton, G., Clement, B., and Okada, M., 2001, Brunhes Epoch magnetic field excursions recorded in ODP Leg 172 sediments: Proceedings of the Ocean Drilling Project, Scientific Results, v. 172 doi:10.2973/odp.proc.sr.172.216.2001
McManus, J.F., Oppo, D.W., Cullen, J.L., and Healey, S., 2003, Marine isotope stage 11 (MIS 11): analog for Holocene and future climate?: American Geophysical Union, Geophysical Monograph 137, p. 69-86.
Meyers, P.A., and Ishiwatari, R., 1995, Lacustrine organic geochemistry – an overview of indicators of organic matter sources and diagenesis in lake sediments: Organic Geochemistry, v. 20, p. 867-900.
Phillips, E.H., Goff, F., Kyle, P.R., McIntosh, W.C., Dunbar, N.W., and Gardner, J.N., in press, $^{40}Ar/^{39}Ar$ age constraints on the duration of resurgence at the Valles caldera, New Mexico: Journal of Geophysical Research.
Prokopenko, A.A., Williams, D.F., Kuzmin, M.I., Karabanov, E.B., Khursevich, G., and Peck, J.A., 2002, Muted climate variations in continental Siberia during the mid-Pleistocene epoch: Nature, v. 418, p. 65-68.
Roberts, A.P., Reynolds, R.L., Verosub, K.L., and Adam, D.P., 1996, Environmental magnetic implications of greigite (Fe_3S_4) formation in a 3 m.y. lake sediment record from Butte Valley, northern California: Geophysical Research Letters, v. 23, p. 2859-2862.
Schnurrenberger, D.S., Russell, J.M., and Kelts, K.R., 2003, Classification of lacustrine sediments based on sedimentary components: Journal of Paleolimnology, v. 29, p. 141-154.
Sears, P.B., and Clisby, K.H., 1952, Two long climate records: Science, v. 116, p. 176-178.
Seigenthaler, U., Stocker, T.F., Monnin, E., Luthi, D., Schwander, J., Stauffer, B., Raynaud, D., Barnola, J-M., Fischer, H., Masson-Delmotte, V., and Jouzel, J., 2005, Stable carbon cycle-climate relationship during the late Pleistocene: Science, v. 310, p. 1313-1317.
Singer, B.S., Relle, M.K., Hoffman, K.A., Battle, A., Laj, C., Guillou, H., and Carracedo, J.C., 2002, Ar/Ar ages from transitionally magnetized lavas on La Palma, Canary Islands, and the geomagnetic instability timescale: Journal of Geophysical Research, v. 107, doi:10.1029/2001JB001613.
Smith, G.A., McIntosh, W., and Kuhle, A.J., 2001, Sedimentologic and geomorphic evidence for seesaw subsidence of the Santo Domingo accommodation-zone basin, Rio Grande rift, New Mexico: Geological Society of America Bulletin, v. 113, p. 561-574.
Smith, G.I., and Street-Perrott, F.A., 1983, Pluvial lakes of the western United States, *in* Wright, H.E. Jr., and Porter, S.C., eds., Late Quaternary environments of the United States, Volume 1: the Late Pleistocene: Minneapolis, University of Minnesota Press, p. 190-214.
Smith, R.L., and Bailey, R.A., 1968, Resurgent cauldrons: Geological Society of America, Memoir 116, p. 613-662.
Smith, R.L. Bailey, R.A., and Ross, C.S., 1970, Geologic map of the Jemez Mountains, New Mexico. U.S. Geological Survey, Miscellaneous Geologic Investigations, Map I-571, scale 1:125,000.
Spell, T.L., and Harrison, T.M., 1993, $^{40}Ar/^{39}Ar$ geochronology of post-Valles Caldera rhyolites, Jemez Mountains volcanic field, New Mexico: Journal of Geophysical Research, v. 98, p. 8031-8051.
Toney, J.L., and Anderson, R.S., 2006, A postglacial paleoecological record from the San Juan Mountains of Colorado: fire, climate and vegetation history: The Holocene, v. 16, p. 505-517.
Winograd, I.J., Coplen, T.B., Landwehr, J.M., Riggs, A.C., Ludwig, K.R., Szabo, B.J., Kolesar, P.T., and Revesz, K.M., 1992, Continuous 500,000-year climate record from vein calcite in Devils Hole, Nevada: Science, v. 258, p. 255-259.
WoldeGabriel, G., Heikoop, J., Goff, F., Counce, D., Fawcett, P.J., and Fessenden-Rahn, J., 2007, Appraisal of post-South Mountain volcanism lacustrine sedimentation in the Valles Caldera using tephra units: New Mexico Geological Society, 58th Field Conference, Guidebook, p. 83-85.